Time-Resolved Synchrotron X-ray Diffraction and Infrared Spectroscopic Studies of Imidization and Structural Evolution in a Microscaled Film of PMDA-3,4'-ODA Poly(amic acid)

ARTICLE *in* LANGMUIR · NOVEMBER 2001

Impact Factor: 4.46 · DOI: 10.1021/la0108656

Time-Resolved Synchrotron X-ray Diffraction and Infrared Spectroscopic Studies of Imidization and Structural Evolution in a Microscaled Film of PMDA-3,4′-ODA Poly(amic acid)

Tae Joo Shin, Byeongdu Lee, Hwa Shik Youn, Ki-Bong Lee, and Moonhor Ree*

Pohang University of Science & Technology, Department of Chemistry, Center for Integrated Molecular Systems, BK21 Functional Polymer Thin Film Group and Polymer Research Institute, and Pohang Accelerator Laboratory, San 31, Hyoja-dong, Pohang 790-784, Republic of Korea

Received June 11, 2001. In Final Form: September 21, 2001

The imidization behavior and structural evolution in a microscaled film of poly(3,4′-oxydiphenylene pyromellitamic acid) precursor are studied by time-resolved synchrotron wide-angle X-ray diffraction and infrared spectroscopy to investigate the relationship between thermal imidization and structural evolution in the precursor. The precursor film displays only short-range order, but its polyimide film shows a crystalline structure based on an orthorhombic crystal lattice unit. When the precursor is heated at 2.0 °C/min, it undergoes imidization over the temperature range 124−310 °C through a *two-step process*: (i) decomplexation of the amide linkage from residual solvent molecules and other intra- and intermolecular amic acid groups and (ii) imide-ring closure. The maximum rate of imidization occurs at 148.4 °C. Anhydride rings are found to form transiently over the range 93−310 °C, which are attributed to the nature of the equilibrium between the precursor and its constituent anhydride- and amino-terminated species. The imidization reaction begins prior to the commencement of structural evolution. The structural evolution takes place over 132−380 °C as a *three-step process*: initiation, primary growth, and secondary growth. In particular, the initiation step requires at least 3.2% imidization. The structural evolution is further influenced by the short-range ordered structure formed in the precursor film in the process of film formation. However, the overall crystallinity in the fully imidized film is limited to only 21.4%.

Introduction

Aromatic polyimides are used as electrical insulators, passivation layers, liquid-crystal alignment layers, gas separation membranes, and matrix resins for fiber-reinforced plastics because of their excellent mechanical, electrical, chemical, and thermal properties.[1] However, most aromatic polyimides cannot be processed because they are insoluble and have a high glass transition temperature.[1] Thus, they are first synthesized in soluble precursor forms and then processed in various ways, before finally being converted to polyimides.[1a−c,2] Poly(amic acid) (PAA) is a representative soluble precursor, which is soluble in *N*-methyl-2-pyrrolidone, dimethyl sulfoxide, and *N*,*N*-dimethylacetamine.[1a−c,2] PAA is usually processed as a film and imidized either thermally or chemically.

For polyimides prepared from PAAs, the morphological structure and properties have been found to strongly depend on the imidization history.[2,3] However, structural analyses have been mostly limited to the morphological structures of polyimides that have already been prepared under particular conditions.[3] Even study of the imidization behavior of PAAs has been limited mostly to polymer samples that had already been imidized. Various thermal analysis techniques have been employed, such as thermogravimetry, conventional and modulated differential scanning calorimetry, and dynamic mechanical thermal analysis, to examine the in situ imidization behavior of PAA precursors.[2] However, each chemical repeat unit in PAAs contains carboxylic acid and amide groups, which can form complexes with solvent molecules via hydrogen bonding. Hence, PAAs always contain some amount of residual solvent. Such residual solvent molecules are evaporated together with the water byproduct generated by imidization. This situation makes it difficult to use thermal analysis techniques to quantitatively determine the imidization behavior of PAAs. In contrast, infrared (IR) spectroscopy avoids such difficulties and has therefore been widely used as a powerful tool for investigating the

* To whom correspondence should be addressed. Tel: +82-54-279-2120. Fax: +82-54-279-3399. E-mail: ree@postech.edu.

(1) (a) *Polyimides*: *Fundamentals and Applications*; Ghosh, M. K., Mittal, K. L., Eds.; Marcel Dekker: New York, 1996. (b) Sroog, C. E. *Prog. Polym. Sci.* **1991**, *16*, 561. (c) Czornyj, G.; Chen, K. J.; Prada-Silva, G.; Arnold, A.; Souleotis, H.; Kim, S.; Ree, M.; Volksen, W.; Dawson, D.; DiPietro, R. *Proc.—Electron. Compon. Technol. Conf.* **1992**, *42*, 682. (d) Lee, K.-W.; Viehbeck, A.; Walker, G. F.; Cohen, S.; Zucco, P.; Chen, R.; Ree, M. *J. Adhes. Sci. Technol.* **1996**, *10*, 807. (e) Kim, S. I.; Ree, M.; Shin, T. J.; Jung, J. C. *J. Polym. Sci., Part A*: *Polym. Chem.* **1999**, *37*, 2909.

(2) (a) Kim, S. I.; Pyo, S. M.; Ree, M. *Macromolecules* **1997**, *30*, 7890. (b) Kim, S. I.; Pyo, S. M.; Kim, K.; Ree, M. *Polymer* **1998**, *39*, 6489. (c) Kim, S. I.; Ree, M.; Shin, T. J.; Lee, C.; Woo, T. H.; Rhee, S. B. *Polymer* **2000**, *41*, 5173. (d) Ree, M.; Kim, K.; Woo, S. H.; Chang, H. *J. Appl. Phys.* **1997**, *81*, 698. (e) Kim, K.; Ryou, J. H.; Kim, Y.; Ree, M.; Chang, T. *Polym. Bull.* **1995**, *34*, 219. (f) Ree, M.; Yoon, D. Y.; Volksen, W. *J. Polym. Sci., Polym. Phys. Ed.* **1991**, *29*, 1203. (g) Brekner, M.-J.; Feger, C. *J. Polym. Sci., Part A*: *Polym. Chem.* **1987**, *25*, 2005. (h) Brekner, M. J.; Feger, C. *J. Polym. Sci., Part A*: *Polym. Chem.* **1987**, *25*, 2429.

(3) (a) Isoda, S.; Shimada, H.; Kochi, M.; Kambe, H. *J. Polym. Sci., Polym. Phys. Ed.* **1981**, *19*, 1293. (b) Kochi, M.; Shimada, H.; Kambe, H. *J. Polym. Sci., Polym. Phys. Ed.* **1984**, *22*, 1979. (c) Russell, T. P. *J. Polym. Sci., Polym. Phys. Ed.* **1984**, *22*, 1105. (d) Takahashi, N.; Yoon, D. Y.; Parrish, W. *Macromolecules* **1984**, *17*, 2584. (e) Ree, M.; Chu, C. W.; Goldberg, M. J. *J. Appl. Phys.* **1994**, *75*, 1410. (f) Krigbaum, W. R.; Sasaki, S. *J. Polym. Sci., Polym. Phys. Ed.* **1981**, *19*, 1339. (g) Factor, B. J.; Russell, T. P.; Toney, M. F. *Macromolecules* **1993**, *26*, 2847. (h) Tony, M. F.; Russell, T. P.; Logan, J. A.; Kikuchiu, H.; Sands, J. M.; Kumar, S. K. *Nature* **1994**, *374*, 709. (i) Arnold, F. E., Jr.; Shen, D.; Harris, F. W.; Cheng, S. Z. D. *J. Mater. Chem.* **1994**, *4*, 105. (j) Liu, J.; Cheng, S. Z. D.; Harris, F. W.; Hsiao, B. S.; Gardner, K. H. *Macromolecules* **1994**, *27*, 989. (k) Cheng, S. Z. D.; Wu, Z.; Eashoo, M.; Hsu, S. L. C.; Harris, F. W. *Polymer* **1991**, *32*, 1803. (l) Ree, M.; Shin, T. J.; Lee, S. W. *Korea Polym. J.* **2001**, *9*, 1.

10.1021/la0108656 CCC: $20.00
Published on Web 11/09/2001

imidization behavior of PAAs.[4] Despite the advantages of IR spectroscopic analysis, it has been restricted to polyimides that were already prepared from PAAs. Furthermore, past work on characterizing structural and imidization behavior has focused mainly on only a few polyimide systems, such as poly(4,4′-oxydiphenylene pyromellitimide) (PMDA-4,4′-ODA) and poly(*p*-phenylene biphenyltetracarboximide) (BPDA-PDA).[2−5]

The time-resolved measurement of the structural evolution during the imidization of PAA precursor has yet to be conducted. A study of this type is critical to determining the mechanism of the structural formation of polyimide and to further understanding the relationship between structure and properties. Imidization behavior has not been previously studied on a time-resolved basis, which is essential to understanding polyimide formation and resultant structure and properties.

We chose to study poly(3,4′-oxydiphenylene pyromellitamic acid) precursor, which can form a crystal structure in the polyimide. First, we investigated its imidization behavior and structural evolution during thermal imidization using time-resolved infrared spectroscopy and wide-angle X-ray diffraction techniques with synchrotron radiation sources, to find the relationship between imidization and structural evolution. The imidization behavior was further investigated by thermogravimetric analysis.

Experimental Section

Materials and Sample Preparation. Pyromellitic dianhydride (PMDA) and 3,4′-oxydiphenylene (3,4′-ODA) were supplied by the Chriskev Co. Anhydrous *N*-methyl-2-pyrrolidone (NMP) was purchased from the Aldrich Co. Poly(3,4′-oxydiphenylene pyromellitamic acid) [PMDA-3,4′-ODA poly(amic acid)] was prepared by slowly adding sublimed PMDA to the purified 3,4′-ODA in NMP (bp 202 °C). Once the dianhydride addition was complete, the reaction flask was capped tightly and stirred for 2 days to completely homogenize the polymerization mixture, giving a PAA solution with a solid content of 13.5 wt % (see Figure 1). The intrinsic viscosity of the precursor polymer was 0.985 dL/g in NMP at 25.0 °C. The PAA solution was spin-coated onto precleaned glass substrates and silicon wafers and dried on a hot plate at 80 °C for 10 min, giving PAA films of thickness 5.5 μm. The residual NMP content of the dried films was determined by ^{1}H NMR spectroscopy to be 32.0 wt %.

Thermogravimetric Analysis. Thermogravimetric analysis (TGA) was carried out under a dried nitrogen gas flow using a Seiko TGA instrument. Dried PAA films with various NMP contents were tested. Each sample was heated to 380 °C at 2.0 °C/min and then further heated to 800 °C at 5.0 °C/min.

Time-Resolved FT-IR Spectroscopic Analysis. FT-IR spectra were measured in transmission mode using an FT-IR spectrometer (Mattson Research Series) equipped with an MCT detector cooled by liquid nitrogen. The spectrometer was calibrated using a polystyrene standard in film. Spectra were recorded using 42 scans at a spectral resolution of 4.0 cm^{-1}. Each dried PAA film, which was coated onto a silicon wafer, was inserted into an IR sample block in which the temperature was controlled by a Eurotherm temperature controller with a K-type thermocouple. The sample block had a nitrogen blowing-hole to protect the sample from oxidation at high temperature. IR spectra were collected as a function of temperature and time while the sample was heated to 380 °C at a rate of 2.0 °C/min.

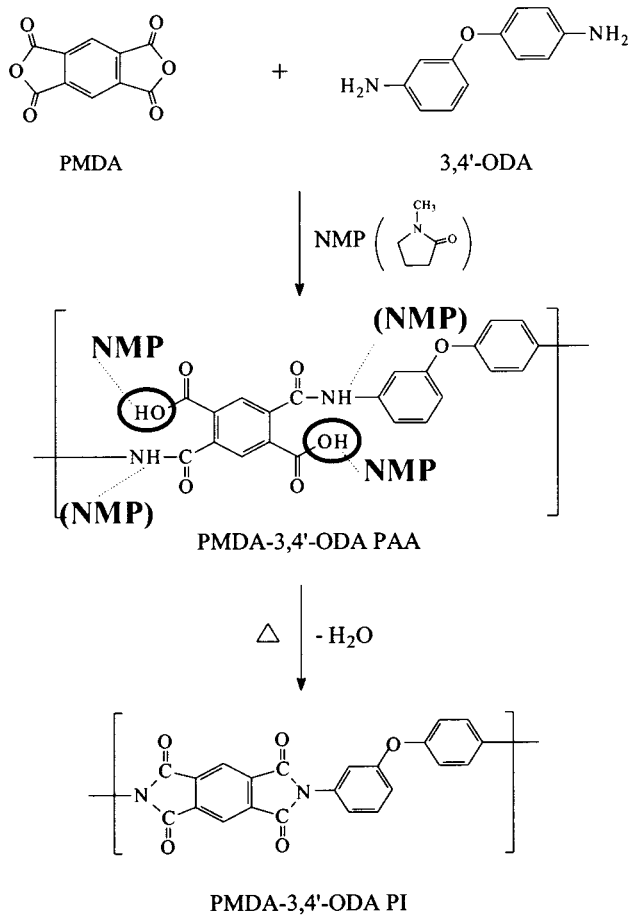

Figure 1. Synthetic scheme of PMDA-3,4′-ODA PI and its complexation with *N*-methyl-2-pyrrolidone (NMP) solvent.

Time-Resolved Wide-Angle X-ray Diffraction. The dried PAA films were cut to a dimension of 5 mm × 5 mm and stacked to give a total thickness of ca. 1.1 mm. Each stack of films was inserted into a square-shaped sample cell with a central 2 mm diameter hole. This sample cell was placed into a sample block and heated to 380 °C at a rate of 2.0 °C/min, maintained at 380 °C for 30 min, and then cooled to room temperature. During this procedure, the wide-angle X-ray diffraction (WAXD) pattern was collected as a function of temperature and time. Each WAXD pattern was measured with an exposure time of 30 s.

Time-resolved WAXD measurements were carried out in transmission mode at the 4C1 beamline[6] of the Pohang Light Source (PLS) facility (2.50 GeV power), Pohang University of Science & Technology. The synchrotron X-ray radiation source had a wavelength of $\lambda = 1.608$ Å. WAXD patterns were measured using a one-dimensional silicon-photodiode array detector (model X/PDA-2048, Princeton Instruments, Inc.). The heating block was controlled using a Eurotherm controller with a K-type thermocouple. The heating block had N_2 blowing-holes to protect the polymer sample from thermal oxidation at high temperature. Another Eurotherm controller with a K-type thin-wire thermocouple was directly contacted to the sample to correctly monitor the sample temperature.

A peak-fitting program (Peakfit, Jandel Scientific) was used to separate the amorphous and crystalline peaks in the measured WAXD patterns. All the diffraction peaks were separated and fitted with Gaussian functions on a single baseline. Based on this analysis method, estimations were made of the Bragg spacing, mean crystallite size, and overall crystallinity. The Bragg spacing, *d*, of each diffraction peak was calculated using the Bragg equation. In general, a diffraction peak from single crystals or crystalline powders becomes broader as the crystal size decreases and the crystal defect level increases. This phenomenon

(4) (a) Ishida, H.; Wellinghoff, S. T.; Baer, E.; Koenig, J. L. *Macromolecules* **1980**, *13*, 826. (b) Kumar, D. *J. Polym. Sci., Polym. Chem. Ed.* **1981**, *19*, 795. (c) Thomson, B.; Park, Y.; Painter, P. C.; Snyder, R. W. *Macromolecules* **1989**, *22*, 4159. (d) Snyder, R. W.; Thompson, B.; Bartges, B.; Czerniawski, D.; Painter, P. C. *Macromolecules* **1989**, *22*, 4166. (e) Krasovskii, A. N.; Antonov, N. P.; Koton, M. M.; Kalnin'sh, K. K.; Kudrysavtsev, V. V. *Polym. Sci. U.S.S.R.* **1979**, *21*, 1038.

(5) Pryde, C. A. *J. Polym. Sci., Polym. Chem. Ed.* **1989**, *27*, 711.

(6) Bolze, J.; Kim, J.; Lee, B.; Shin, T. J.; Huang, J.-Y.; Rah, S.; Lee, J. M.; Youn, H. S.; Ree, M. *Res. Macromol. Res.*, in press.

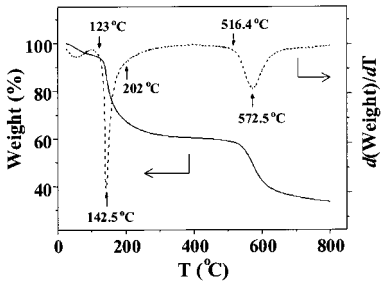

Figure 2. TGA thermogram and its first derivative for PMDA-3,4′-ODA PAA. The measurement was conducted under a nitrogen atmosphere. The heating rate was 2.0 °C/min until 380 °C and thereafter 5.0 °C/min.

provides an experimental method for determining the size of, and defect level in, submicroscopic crystals. For a sample composed of relatively perfect crystallites, the mean crystallite dimension L_c perpendicular to a (hkl) plane is given by the Scherrer equation.[7] In addition, the degree of overall crystallinity, X_c, is estimated from the integrated intensities of the crystalline diffraction peaks and the amorphous halo peaks. Although the measured value of X_c may differ from the true value because of defects in the crystal lattice and thermal disorder, we adopt this value as an apparent crystallinity.

Results and Discussion

TGA Analysis. TGA analysis was conducted on the dried PAA films of thickness 5.5 μm that contained 32.0 wt % NMP. A typical TGA thermogram is illustrated in Figure 2, which gives the weight loss and its first derivative measured while heating the PAA film. The PAA displays a three-step weight loss behavior below 380 °C. The first step appears below 123 °C and involves a relatively small weight loss, which is probably due to the decomplexation of NMP molecules bound via hydrogen bonding to the amide linkages and carboxylic acid groups of the PAA precursor chains. The second step occurs over the temperature range 123−202 °C and involves a large and rapid weight loss. This significant weight loss might be due to the removal of the decomplexed NMP solvent and the water byproduct of the imide-ring closures of the PAA polymer chains being imidized. In addition, the minimum in the plot of d(Weight)/dT versus T appears at 142.5 °C, indicating that the highest rate of weight loss occurs at that temperature. The third step occurs over the range 202−380 °C and shows a very small weight loss with a slow rate, which might result from the dehydration of the partially imidized precursor chains that are still undergoing imide-ring closure with a slow imidization rate.

Beyond the three steps of weight loss described above, another significant weight loss appears in the temperature region higher than 516.4 °C, which is due to the decomposition of the imidized polymer chains.

From the results, it is concluded that in the heating run the PAA precursor simultaneously commences both decomplexation from NMP molecules and imidization at around 123 °C and then undergoes the majority of imidization over the range 123−202 °C, but the completion of imidization requires thermal heating to >202 °C.

Time-Resolved FT-IR Spectroscopic Measurements. Time-resolved FT-IR spectroscopic investigation was carried out during the thermal imidization of the precursor film under the same conditions as the TGA measurement described above.

(7) (a) Scherrer, P. *Gottinger Nachrichten* **1918**, *2*, 98. (b) Klug, H. P.; Alexander, L. E. *X-ray Diffraction Procedures;* Wiley: New York, 1954.

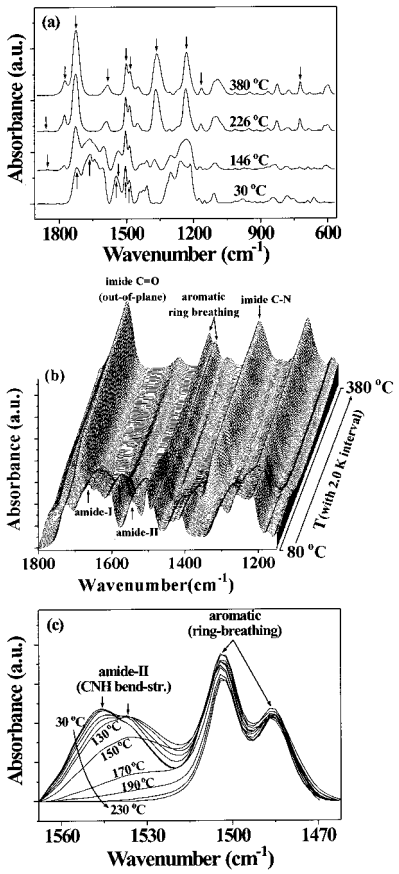

Figure 3. IR spectra measured during thermal imidization of PMDA-3,4′-ODA PAA at a rate of 2.0 °C/min. Part a shows the IR spectra measured at the indicated temperatures on the heating run. Part b displays typical IR spectra monitored during the imidization as a function of temperature. Part c shows vibrational characteristics of amide-II (−CNH− bend−stretch) and aromatic ring (ring-breathing) monitored over 30−230 °C as a function of temperature.

Figure 3a shows typical IR spectra taken at three different temperatures during imidization. Some characteristic IR peaks can be assigned in these spectra with the aid of previously reported results for PMDA-4,4′-ODA PAA and its polyimide and model compounds,[4] as well as BPDA-PDA PAA and its polyimide.[5]

In the spectrum of the PAA precursor measured at 30 °C, the peak centered at 1722 cm^{-1} is assigned to the stretching of the carbonyl (−CO−) in the carboxylic acid group, while the peak centered at 1662 cm^{-1} is assigned to the vibrational characteristics of amide-I (i.e., stretching of the carbonyl (−CO−) in the amide linkage). The two peaks at 1545 and 1536 cm^{-1} are assigned to the vibrational characteristics of amide-II (−CNH− bend−stretch). In addition, the two peaks at 1508 and 1489 cm^{-1} are assigned to the ring-breathing modes of the para- and meta-substituted benzene rings in the 3,4′-ODA unit, respectively. Last, the peak at 1597 cm^{-1} corresponds to the quadrant stretch of carbon-to-carbon double bonds in the aromatic ring, which overlaps in part with the vibrational peaks of amide-I.

On the other hand, for the spectrum of the imidized polymer at 380 °C, the two peaks at 1774 and 1725 cm^{-1} are assigned to the in-phase and out-of-phase stretching vibrations of the imide carbonyl (−CO−), respectively. The single peak at 1363 cm^{-1} is assigned to the −CN− stretch in the imide ring, while another peak at 722 cm^{-1} is assigned to the bending mode of the carbonyl in the imide ring. In addition, both the aromatic ring-breathing

modes and the quadrant stretch of −C═C−, which are observed in the PAA precursor, are detected in the polyimide. The asymmetric stretch of −COC− in the 3,4′-ODA unit is clearly detected at 1231 cm^{-1}.

Figure 3b illustrates representative IR spectra measured in situ during the imidization of the PAA precursor. In the imidization run, the characteristic peaks of amic acid groups (carboxylic acid, amide-I, and amide-II) vary slightly with temperature even before the imidization reaction begins. However, when the imidization reaction begins, these vibrational peaks decrease drastically with increasing temperature, while the characteristic peaks of the imide ring appear and become stronger with increasing temperature. To quantitatively investigate the imidization behavior of the PAA precursor, the following characteristic peaks have been separated from each IR spectrum and their peak areas have been plotted as a function of temperature: amide-II and anhydride carbonyls as well as imide carbonyl and −CN− linkage. The estimated peak maxima and peak areas, normalized to their respective maximum values, are plotted in Figure 4 as a function of temperature. These plots are discussed in detail in the following.

Figure 4a shows the temperature dependence of the amide-II peak area. The drastic drop in area over 124−210 °C is attributed to the consumption of amide linkages by imide-ring formation. This indicates that the imidization reaction takes place mainly in the temperature range 124−210 °C in the heating run. The amide-II peak is still detected up to 310 °C, although its intensity is very weak. This indicates that the imidization reaction continues until 310 °C.

In addition, a small drop in the amide-II peak is observed in the range 70−110 °C, where imidization is not yet involved. The amide-II feature appears as two vibrational peaks rather than a single peak [see Figure 3c]. The two peaks vary with temperature. For the dried precursor film, a main peak is observed at 1545 cm^{-1} with a shoulder peak at 1536 cm^{-1}. However, on elevating the temperature to 100 °C, the high-frequency peak weakens whereas the low-frequency peak becomes more intense. The two peaks reach almost equivalent intensity at 100 °C and maintain that level up to 124 °C. When the imidization reaction takes place above 124 °C, the high-frequency peak weakens further, becoming a shoulder, and the low-frequency peak strengthens, becoming the main peak. The overall intensity of the two peaks decreases with elevating temperature because of the conversion of amide linkages to imide rings.

In fact, the amide linkage in PAA has been found to form complexes with residual NMP solvent[2] and other amic acid groups both intra- and intermolecularly[4c] via hydrogen bonding. In the heating run, residual NMP molecules are evaporated out continuously with increasing temperature. Furthermore, such hydrogen bonds weaken with elevating temperature because they are in equilibrium with their constituents. Thus, the two amide-II peaks, as well as their intensity variations, originate from the complexation process of amide linkages with residual NMP molecules and other amic acid groups. The high-frequency peak is due to amide linkages complexed with NMP molecules and other amic acid groups, whereas the low-frequency peak results from amide linkages that are for the most part free from NMP and other amic acid groups. Conclusively, the intensity drop in the range 70−100 °C is caused by the complexation-to-decomplexation transition of amide linkages with NMP and other amic acid groups and subsequent NMP evaporation. Furthermore, amide linkages undergo imidization through a two-step process, decomplexation from NMP and other amic acid groups followed by imide-ring closure.

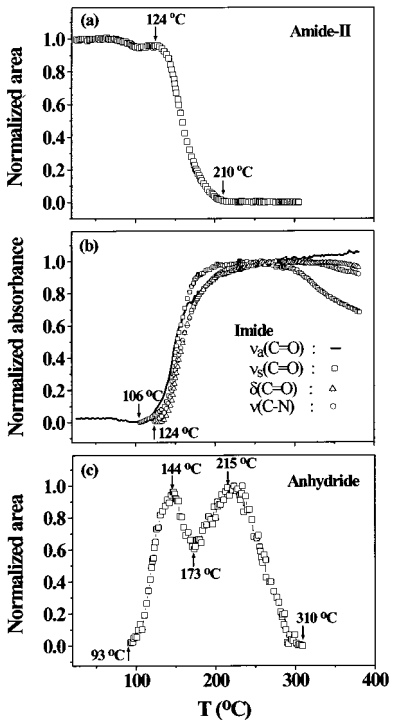

Figure 4. Intensity and peak area variations of some characteristic vibrational bands measured during thermal imidization of PMDA-3,4′-ODA PAA at a rate of 2.0 °C/min. Parts a and c show the temperature dependence of the amide-II (−CNH− bend−stretch) peak area and of the anhydride peak area, respectively. Part b displays variations of the vibrational peaks of the imide ring as a function of temperature: —, ν_a(CO) (−CO− out-of-phase stretch); □, ν_s(CO) (−CO− in-phase stretch); △, δ(CO) (−CO− bend); ○, ν(C−N) (−C−N− stretch).

Figure 4b illustrates both the −CN− stretch and −CO− bend of the imide ring, which vary with temperature. These bands first appear at 124 °C, after which their peak intensities rapidly increase with increasing temperature up to 210 °C. Thereafter, they slowly increase, reaching their maximum values at 310 °C. Similarly, the −CO− in-phase stretching peak of the imide ring first appears at 106 °C, after which its peak intensity increases drastically with increasing temperature up to 210 °C before slowly reaching its maximum at 310 °C. In addition, the −CO− out-of-phase stretching peak of the imide ring shows similar behavior in the peak area versus temperature plot to that observed for its in-phase stretching peak. However, it is noteworthy how the analysis of the peak was done. This peak in the imide ring overlaps fully with the stretching vibration of carbonyl in the carboxylic acid group of the PAA precursor. Thus, the initial peak area measured at 30 °C is subtracted from all the measured peak areas.

Above 310 °C, the peaks of both the −CN− stretch and the −CO− bend decrease slowly with increasing temperature, while the −CO− in-phase stretching peak drops substantially as the temperature is raised. In contrast, the −CO− out-of-phase stretching peak increases with temperature. These variations may be due to a temperature dependence in their absorption coefficients or to their orientations with respect to the film plane. The orientation effect arises because the samples were monitored in transmission mode in the IR measurement in which the electric vector of the IR beam is in the film plane. In addition, it is well-known that rigid and semirigid

aromatic polyimides in thin films exhibit large out-of-plane birefringence due to their high in-plane orientations taking place through the imidization process.[2d,3a−e] Such in-plane chain orientation may occur favorably in the thin film of the PMDA-3,4′-ODA PAA precursor which undergoes imidization because of the semirigid chain characteristic of the resulting polyimide. Indeed, both the −CN− and the −CO− vibrations monitored in this study might be influenced by in-plane orientation of the polymer chains occurring in the thin film. The −CO− bond of the imide ring is a side group, whereas the −CN− bond is a part of the backbone, causing the −CO− stretching and bending peaks to be sensitive to orientation of the imide ring itself, compared to the −CN− stretching peak. However, the axes of −CN− bonds in the in-plane oriented polyimide chain need not necessarily be parallel to the polymer chain axis, because the polyimide having one ether linkage per chemical repeat unit on the backbone is a kinked polymer chain rather than a fully rodlike one. Taking into account these aspects, the variations of the −CN− and −CO− vibrational peaks observed above 310 °C reflect that the state of molecular orientation gradually changes further above that temperature.

As described above, one may use all five vibrational peaks from the amide-II and imide ring to determine the degree of imidization [see Figure 4a,b]. However, the −CNH− bend−stretching peak of amide-II is sensitive to the content of residual solvent, because it is affected by complexation with the solvent. Furthermore, this peak is influenced by hydrogen bonding with other amide and carboxylic acid groups. Such complexation and hydrogen bonding are influenced by temperature, causing the stretching peak to be changed further by variations in the temperature. These factors cause some errors in the determination of the peak area, which is critical for estimating the degree of imidization. On the other hand, the imide carbonyl peak in the out-of-phase stretching mode overlaps fully with the carbonyl stretching peak in the carboxylic acid of the PAA precursor, as mentioned above. In addition, both in-phase stretching and bending peaks in the imide carbonyl overlap in part with those of the carbonyl of the anhydride group that forms transiently during the heating run. The formation of the anhydride group is discussed in detail below. These carbonyl peaks may change further, depending on the in-plane orientation of the imide ring in the thin film. All of the factors mentioned above cause errors in the estimation of the peak intensities and areas.

In contrast, the stretching peak of −CN− in the imide ring is free from overlap with other peaks and is less sensitive to in-plane orientation of the imide ring. *Monitoring the imide −CN− peak therefore proved to be the most valuable way of determining the degree of imidization.*

The degree of imidization ($X_{\text{Imidization}}$) was determined from the plot of the imide −CN− peak versus temperature. As illustrated in Figure 5, the precursor film starts to imidize at 124 °C and has undergone 93.5% imidization by 210 °C, finally reaching 100% imidization at 310 °C. If any small amount of precursor chains or unimidized segments remain, they should undergo imidization upon further heating to 380 °C and soaking at that temperature.

Figure 5 presents a plot of $d(X_{\text{Imidization}})/dT$ versus T, which shows a maximum at 148.4 °C. This indicates that the imidization reaction takes place with a maximum rate at that temperature. As mentioned above, the weight loss with temperature in the TGA analysis gives the maximum rate of weight loss at 142.5 °C. These results suggest the following. First, the imidization process in the precursor

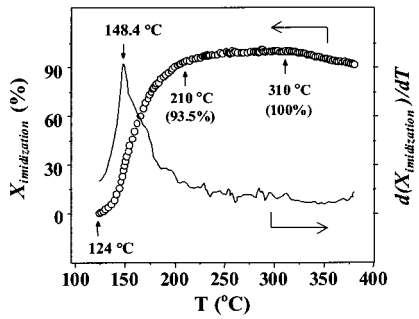

Figure 5. Degree of imidization and its derivative as estimated from the variation of the imide −CN− stretching band measured during thermal imidization of PMDA-3,4′-ODA PAA at a rate of 2.0 °C/min.

is closely related to its decomplexation from residual NMP molecules and other amic acid groups. The decomplexed NMP molecules evaporate from the film sample, apparently leading to a maximum rate of weight loss at 142.5 °C. Second, the decomplexation and evaporation of residual NMP molecules immediately initiates and accelerates the imidization of the precursor polymers, and the imidization proceeds with a maximum rate at 148.4 °C. In addition, the evaporation of water byproduct generated by the imidization contributes to the weight loss. Finally, the decomplexed solvent molecules may act as plasticizers in the polymer film until they evaporate out. Such plasticization makes the precursor polymer chains more mobile, facilitating their imidization.

Beyond the IR peaks associated with the PAA precursor and its polyimide discussed above, another weak peak appears at around 1856 cm^{-1} and disappears later during the heating run (see IR spectra measured at 146 and 226 °C in Figure 3a). It has been reported that saturated anhydride in a five-membered ring absorbs near 1780 and 1860 cm^{-1}, whereas conjugated anhydride in a five-membered ring absorbs near 1760 and 1850 cm^{-1}.[8] The band at the lower wavenumber is much more intense in both cases.[8] Therefore, the weak band at 1856 cm^{-1} is assigned to an anhydride ring that is formed transiently during the heating run. The strong band associated with this moiety is also expected to appear at around 1760−1780 cm^{-1}. However, it overlaps to a great extent with the carbonyl in-phase stretch of the imide ring that is formed through the imidization process.

Anhydride-ring formation has previously been reported for partially imidized PMDA-4,4′-ODA PAA films by Snyder et al.[4d] and for partially imidized BPDA-PDA PAA and poly(4,4′-oxydiphenylene-*co*-*m*-phenylene benzophenonetetracarboxamic acid) (BTDA-ODA/MPDA PAA) films by Pryde.[5] However, in these studies the anhydride-ring formation was not investigated in detail. Thus, in the present study we examined the anhydride-ring formation in greater detail.

The peaks at higher wavenumbers due to the anhydride ring are relatively weak (see Figure 3a,b); hence, this part of the spectra is magnified in Figure 6. Their total peak area is also plotted with temperature in Figure 4c and compared with those of amide-II and imide peaks (see Figure 4a,b).

As shown in Figure 4c and 6, the anhydride ring is not detected below 93 °C. This suggests that anhydride groups

(8) (a) *Introduction to Infrared and Raman Spectroscopy*; Colthup, N. B., Daly, L. H., Wiberiey, S. E., Eds.; Academic: New York, 1996. (b) Dauben, W. G.; Epstein, W. W. *J. Org. Chem.* **1959**, *24*, 1595. (c) Bellamy, L. J.; Connelly, B. R.; Philpotts, A. R.; Williams, R. L. *Z. Elektrochem.* **1960**, *64*, 563.

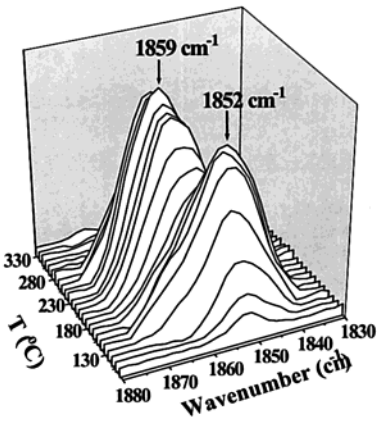

Figure 6. IR spectra of the anhydride ring formed transiently during thermal imidization of PMDA-3,4′-ODA PAA at a rate of 2.0 °C/min.

are present either in an open form such as carboxylic acid or with very low concentration, not enough to be detected in the IR spectroscopy at temperatures less than 93 °C. However, anhydride-ring formation is first detected at 93 °C, which is much lower than the onset temperature of imidization (124 °C). Here, its characteristic vibration appears at 1852 cm^{-1} as a single peak rather than two peaks, which corresponds to conjugated anhydride in a five-membered ring. This peak becomes more intense with increasing temperature up to 144 °C and then weakens with further heating, finally disappearing at around 300 °C (see Figure 6). In addition to the single peak, a new shoulder peak appears at 124 °C, the temperature at which imidization begins (see Figure 6). This shoulder peak is centered at 1859 cm^{-1}, which corresponds to saturated anhydride in a five-membered ring. The intensity of the shoulder peak increases with temperature until 173 °C. Thereafter, the peak changes from a shoulder peak to the major peak and continues to grow with further heating, reaching a maximum at 215 °C. The peak then declines with increasing temperature and finally disappears at 310 °C.

These results give the following information about anhydride formation and its correlation to imidization of the precursor polymer. First, anhydride-ring formation commences at 93 °C, which is lower than the onset temperature of imidization, and continues until the imidization reaction is complete. This anhydride-ring formation may originate from the nature of the polycondensation reaction used to obtain the PAA precursor. Because this polycondensation is an equilibrium reaction, the PAA precursor may undergo a reversible reaction when heated, generating the respective anhydride- and amine-terminated species. This reversible reaction begins at 93 °C, even in the dried PAA film, generating anhydride-terminated species. The conditions are more favorable for this reversible reaction with raising the temperature to 215 °C, where the majority of imidization has already occurred (about 94% imidization). Second, two types of anhydride ring are detected: conjugated and saturated anhydride in a five-membered ring. The occurrence of these two types may be closely related to the presence of residual NMP solvents and of amic acid groups, as well as their stabilities with changing temperature. Formation of the conjugated anhydride is found to be favored at lower temperatures (<173 °C) and in systems with relatively large amounts of residual solvent and amic acid groups. These facts suggest that when the anhydride ring forms it makes a complex with residual NMP molecules and amic acid groups, which is more favorable at lower

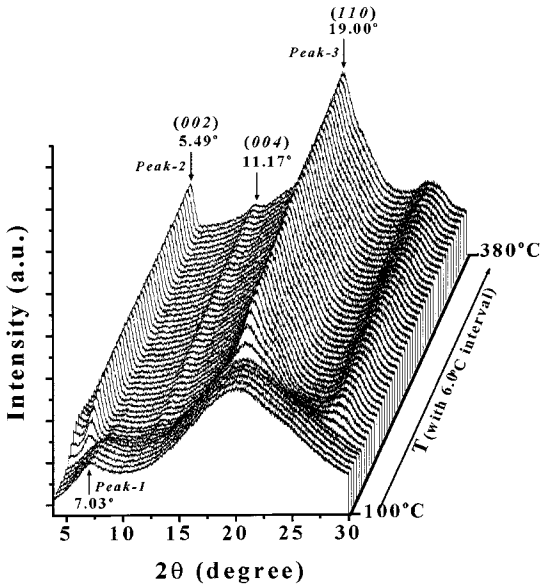

Figure 7. Representative WAXD patterns measured during thermal imidization of PMDA-3,4′-ODA PAA at a rate of 2.0 °C/min. Here, peak 1 at 7.03° (2θ) arises from the chemical repeat units of the PAA precursors in an ordered state, and its *d*-spacing is 13.11 Å which may correspond to the repeat unit length projected along the polymer chain axis. Peak 2 at 5.49° is assigned as (002) diffraction according to the structural analysis reported previously,[9] which has 16.79 Å *d*-spacing corresponding to the chemical repeat unit length of the polyimide projected along the fully extended polymer chain axis. Peak 3 at 19.00° (4.87 Å) is assigned to (110) diffraction which arises from the lateral molecular ordering. The other peak at 11.17° is assigned by (004) diffraction.

temperatures, consequently stabilizing the formation of a conjugated five-membered ring. In contrast, at higher temperatures the anhydride ring has less chance of forming a complex with NMP and amic acid groups because the contents of residual NMP (bp 202 °C) and amic acid groups are very small or no longer available. Furthermore, complexation with NMP and amic acid groups delivers only a small or negligible thermodynamic gain to its stability at higher temperature. Thus, the saturated anhydride ring is more favorable at higher temperatures (>173 °C). The conjugated and saturated anhydrides may be in equilibrium, and the equilibrium constant for transformation between the structures varies with temperature as well as contents of residual NMP and amic acid groups.

Time-Resolved WAXD Measurements. Time-resolved WAXD measurements were carried out on PAA films being imidized under the same conditions as those used for both the TGA and IR spectroscopic measurements. Representative X-ray patterns from these measurements are shown in Figure 7.

The PAA film at room temperature gives two main diffraction peaks, one centered at 7.03° (2θ) and another centered at 20.40°. The peak in the low angle region (peak 1) is relatively weak and broad. Its *d*-spacing is 13.11 Å, which is close to the chemical repeat unit length projected along the axis of the fully extended precursor chain, which is estimated to be ca. 16.9 Å. This diffraction might therefore arise from the repeat distances along the polymer chain. The appearance of peak 1 is an indication that *short-ranged molecular order* exists in the PAA film. The other peak in the high-angle region is very broad and large, indicative of an amorphous halo. This peak has a *d*-spacing of 4.54 Å, which arises from the mean distance between the precursor chains. These results suggest that the PAA

film consist of two phases, which are an amorphous phase in a major portion and a short-range-ordered phase in a minor portion. A similar structure was reported previously for PMDA-4,4′-ODA PAA in a dried film.[3d]

In contrast to the PAA film, its polyimide film reveals a crystal-like X-ray pattern. For example, the film imidized at 380 °C shows several diffraction peaks over 3−30° (2θ): 5.49°, 11.17°, 17.10°, 19.00°, 20.37°, and 27.87°. These diffraction peaks can be assigned according to the structural refinement analysis used previously.[9] The crystalline structure of PMDA-3,4′-ODA polyimide is known to be an orthorhombic crystal lattice. The peak assignments are presented in Figure 7. In particular, the (002) diffraction at 5.49° (peak 2) is estimated to have a *d*-spacing of 16.79 Å, which corresponds to the fully extended length of one chemical repeat unit, and an L_c value of 97 Å. The (110) diffraction at 11.17° (peak 3) has a 4.87-Å *d*-spacing and a 59-Å L_c. These results suggest that the crystalline phases consist of approximately 6 chemical repeat units along the chain axis and approximately 12 polymer chains in the lateral direction. Furthermore, the appearance of the (004) and (210) diffractions supports the existence of such crystalline phases in the polyimide film. Therefore, for the structure being thermally developed from the PAA precursor, we can obtain information about molecular ordering along the polymer chain axis from peak 2 and about lateral chain ordering from peak 3.

Using the structural results above, the time-resolved X-ray patterns were further analyzed in detail to quantitatively investigate the structural evolution occurring in the PAA film undergoing imidization. The characteristic diffraction peaks (namely, peak 1 and peak 2) of the PAA and its polyimide have been separated from each WAXD pattern, and their peak areas have been plotted as a function of temperature in Figure 8a. In this figure, the estimated peak areas have been normalized to the peak area of peak 2 at 380 °C.

The intensity of peak 1 increases with increasing temperature up to 89 °C and then levels off, maintaining that level to just below 124 °C, where the imidization reaction begins. This growth in peak 1 indicates that the structural ordering in the PAA film is enhanced by heating, even though such structure was poorly developed in the film formation process. In fact, the PAA film contains some NMP (32 wt %) as residual solvent. The NMP molecules are complexed with the amide and carboxylic acid groups in the PAA. When the PAA is heated, the NMP molecules partly decomplex from the PAA precursor and evaporate out, as discussed above [see Figure 3c]. Therefore, the structural enhancement might be attributable to the NMP decomplexation and evaporation that occur during the heating run.

When the imidization reaction begins at 124 °C, however, peak 1 drops sharply with increasing temperature and levels off at around 158 °C, at which point the imidization reaction has taken place with only a 47.5% yield. After this point, the weakened peak intensity further declines very slowly with elevating temperature until near 380 °C, which results from further imidization reaction.

In contrast, the characteristic diffraction of the polyimide, peak 2, first appears at 132 °C, which is 8 °C higher than the onset temperature for imidization (124 °C). The imidization reaction at 132 °C has proceeded only 3.2%. After this temperature, the peak 2 intensity rises rapidly with increasing temperature, reaching the first maximum

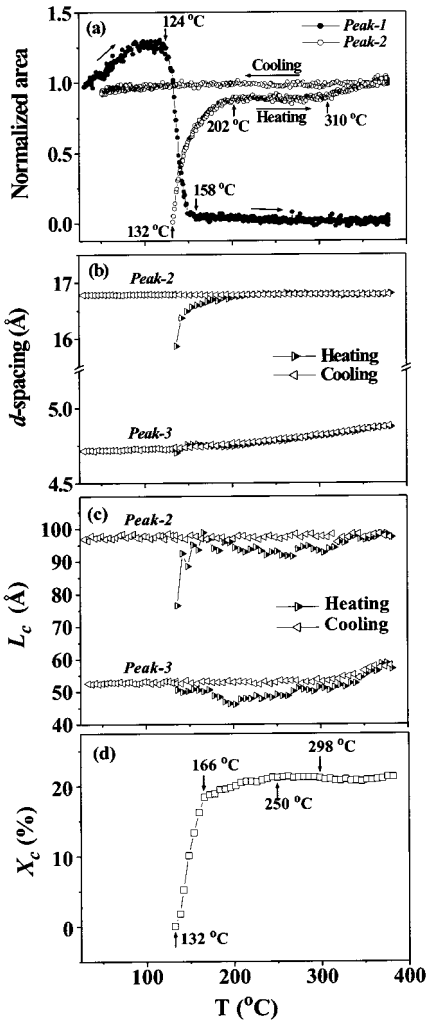

Figure 8. Peak areas, *d*-spacings, and coherence lengths (L_c) of characteristic X-ray diffractions and overall crystallinity measured during thermal imidization of PMDA-3,4′-ODA PAA at a rate of 2.0 °C/min and subsequent cooling. Part a displays the temperature dependence of peak 1 (PAA) areas (●) and of the peak 2 (polyimide) area (○). Part b shows variations in the *d*-spacings of peak 2 and peak 3 from the resulting polyimide as a function of temperature. Part c presents variations in the L_c values of peak 2 and peak 3 from the resulting polyimide as a function of temperature. Part d shows the temperature dependence of the overall crystallinity, which was estimated from the measured X-ray diffraction pattern.

at around 202 °C, where the imidization reaction has taken place with a 91.0% yield. This peak intensity level is maintained until the imidization reaction is complete at 310 °C and thereafter increases again with elevating temperature.

In addition to the intensity variations in peak 2, the peak becomes narrow in shape as temperature increases as shown in Figure 7. Further the peak shows its position shifting to the low-angle region particularly in the early stage (132−200 °C) of the heating run. The *d*-spacing and coherence length L_c of peak 2 have been estimated and plotted with temperature in parts b and c of Figure 8, respectively. The *d*-spacing is 15.80 Å at 132 °C but increases rapidly with increasing temperature and reaches a maximum of 16.79 Å at 202 °C; it then remains at that level until 380 °C. This *d*-spacing value corresponds to the fully extended length of one chemical repeat unit that is projected along the chain axis and is retained through the subsequent cooling run. On the other hand, L_c is 76 Å at 132 °C and then increases very rapidly with elevating

(9) (a) Ree, M.; Nunes, T. L.; Czornyj, G.; Volksen, W. *Polymer* **1992**, *33*, 1228. (b) Ree, M.; Volksen, W.; Yoon, D. Y. To be published. (c) Shin, T. J.; Lee, B.; Ree, M. To be published.

temperature, reaching a maximum of 99 Å at 158 °C. Thereafter, L_c decreases very slightly with temperature. However, it begins to increase at around 310 °C and continues slowly increasing with further elevation of the temperature, finally reaching 97 Å at 380 °C. This L_c level is retained through the entire cooling process.

Peak 3, which results from the characteristic lateral ordering of the polyimide chains, also begins to appear at 132 °C, where peak 2 appears. Peak 3 develops further with increasing temperature, becoming intense and sharp (see Figure 7). In addition, its position shifts to the low-angle region with increasing temperature. Parts b and c of Figure 8 show the variations in *d*-spacing and L_c for peak 3, respectively. The *d*-spacing is 4.70 Å at 132 °C and increases rapidly with temperature until about 158 °C. Thereafter, the *d*-spacing increases continuously with elevating temperature, finally reaching a value of 4.87 Å at 380 °C. In the subsequent cooling run, the *d*-spacing gradually decreases with temperature, finally reaching 4.72 Å at room temperature. On the other hand, the value of L_c is 51 Å at 132 °C and then varies from 46 to 52 Å over the temperature range 132−310 °C. When the temperature is increased further, however, L_c increases again with a steeper slope, reaching 59 Å at 380 °C. In the subsequent cooling, L_c decreases gradually from 59 Å at 380 °C to 54 Å at 310 °C and then maintains that level down to room temperature.

Figure 8d presents the variation of overall crystallinity (X_c) with temperature, which has been estimated from the X-ray diffraction patterns measured at ≥132 °C. The value of X_c increases rapidly to 18.4% at 166 °C, where the imidization yield is 61%. It increases further with increasing temperature and reaches a maximum value (21.3%) at around 250 °C, where the imidization reaction has a 98.5% yield. This X_c value is retained until 292 °C. Thereafter, it decreases very slightly up to 345 °C where it increases again and reaches a maximum value at 380 °C.

From the WAXD results, we can draw the following conclusions about the evolution of crystalline structure and its correlation to the imidization reaction. First, the evolution of the crystalline structural is a *three-step process*: initiation, primary growth, and secondary growth. Crystallization commences at 132 °C, where only 3.2% of imidization has occurred. The primary crystallization takes place immediately thereafter, and its major contribution is made by 202 °C, where imidization has a yield of 91.0%. The secondary crystallization begins at 310 °C, at which the imidization reaction is complete, and continues with temperature up to 380 °C. The onset temperature of the secondary crystallization may be related to the onset temperature of the glass transition ($T_{g(onset)}$) in the imidized film. That is, the secondary crystallization may take place favorably above $T_{g(onset)}$, even though polymer chain mobility is limited because of chain stiffness.

Second, the structural evolution seems to need at least 3.2% imidization to be detectable by WAXD. This leads to a time (or temperature) lag after the commencement of imidization. Therefore, for the thermal imidization process with 2.0 °C/min, the onset temperature of structural evolution is 132 °C rather than 124 °C, the onset temperature of imidization.

Third, the imidization reaction in the PAA film may take place randomly in the ordered phase as well as in the amorphous phase. On the basis of this circumstance, the transformation of the PAA chains in the ordered phase into the crystalline polyimide phase would occur more rapidly than the transformation of the PAA chains in the amorphous phase through the imidization process. Of course, the PAA chains being imidized in the amorphous PAA phase can undergo formation of the crystalline structure but take a relatively longer time. Therefore, the evolution of crystalline structure in the PAA film being imidized might depend on the history of the molecular ordering in the preparation of the precursor film. That is, the molecular order formed in the PAA film may act as nuclei in the crystallization of the polymer chain segments being imidized.

Fourth, peak 1 weakens above 158 °C but is still detected near 380 °C. Here, one can imagine that such a peak detected even at the high temperatures is originated from any incompletion of imidization in the film. As discussed earlier, the in situ IR measurements, however, proved that the imidization reaction is complete at 310 °C. Further, in the measurement of such imidization reaction the IR spectroscopy has much higher sensitivity and resolution than does the X-ray diffraction. So, this possibility can be negligible, which cannot be detectable to the X-ray diffraction measurement. Indeed, such peak observation may be related to the following factors. Short-ranged structural ordering formed in the PAA may be necessary to the formation of the crystalline polyimide structure through the imidization reaction. Alternatively, once short-range-ordered structure was formed in the PAA, its memory, even though its quantity is relatively small, may remain transiently even after the imidization reaction is complete, which may depend on heating (or annealing) temperature and time above 310 °C.

Fifth, it is established that the ultimate *d*-spacing of peak 2 arises from the molecular ordering along the chain axis, at least at 202 °C where 91.0% imidization has been accomplished. Once the ultimate *d*-spacing is achieved, it does not vary further with temperature, regardless of further heating and subsequent cooling. This indicates that the molecular order along the chain axis neither expands nor contracts.

Sixth, the peak associated with molecular ordering along the lateral direction, peak 3, shows a continuous variation of its *d*-spacing with changing temperature. This provides a clear indication that the molecular order thermally expands and contracts in the lateral direction. Its thermal expansion coefficient is estimated to be 61 ppm/°C over 25−200 °C and 158 ppm/°C over 310−380 °C.

Seventh, both L_c (peak 2) and L_c (peak 3) fluctuate over the temperature range 158−310 °C, which may originate from the evolution of the molecular ordering in the dynamic state caused by the gradual imidization of the PAA precursor chains. Furthermore, the fluctuations may be related to the T_g of the PAA film being imidized. When the PAA film is involved in the imidization reaction, its T_g suddenly jumps to a temperature higher than its imidization temperature, depending on its degree of imidization, until ultimately reaching the T_g of the fully imidized polymer. Thus, the PAA film being imidized in the heating run is always in a temporarily frozen state that can restrict chain motion.

Eighth, the peak 2 intensity arises rapidly with temperature over the range 132−202 °C and reaches the first maximum value at 202 °C, then maintaining that level until 310 °C at which the imidization reaction is complete. Above 310 °C, the peak intensity increases again with elevating temperature. Its L_c also increases again with temperature. The peak intensity and L_c increases may result first from the secondary crystallization aforementioned, which occurs favorably above the $T_{g(onset)}$ (=310 °C). In this study, the X-ray diffraction measurements have been conducted in transmission mode in which the

scattering vector is in the film plane, giving structural information only in the film plane. Thus, these increases may also be contributed from enhancement in the in-plane chain orientation taking place favorably above 310 °C, which has been discussed previously in the IR measurement section.

Finally, a thermal-imidization-induced structural evolution has clearly been observed in the polyimide film prepared from the PAA precursor, but the overall crystallinity is limited to only 21.4%. This low crystallinity may be attributed to relative large chain stiffness and high $T_{g(onset)}$ of the resulting polyimide, which are able to provide only limited chain mobility and temperature window to the structural evolution and growth.

Conclusion

Time-resolved WAXD and FT-IR spectroscopic measurements were made for PMDA-3,4′-ODA PAA in a microscaled thin film which was undergoing thermal imidization and subsequent cooling. The measurement results were interpreted taking into consideration the role of the residual NMP solvent, amic acid to amic acid interaction, imidization kinetics, and imidization-induced structure formation. The following conclusions are drawn from this work.

First, the amide-II vibration was found to be sensitive to the complexation and decomplexation of amide linkages with residual NMP solvent and other amic acid groups of the PAA as well as imidization. Thus, the amide-II peak was successfully utilized as a good analytical probe to examine the imidization mechanism of the precursor. It turns out that the PAA precursor undergoes a *two-step imidization reaction*. Namely, the amide linkage in the precursor backbone does decomplex first from the residual NMP solvent and the other amic acid groups, prior to the onset of imidization, and then undergoes imide-ring formation.

Second, among all vibrational peaks of the amic acid group and imide ring, the imide −CN− stretching band was found to be the most valuable probe in determining the degree of imidization.

Third, in the heating run at 2.0 °C/min the PAA begins to imidize at 124 °C and undergoes the majority of imidization up to 210 °C. Imidization then slowly proceeds until it is complete by 310 °C. The maximum rate of imidization occurs at 148.4 °C.

Fourth, in addition to imide-ring formation, anhydride rings are found to form in the range 93−310 °C during imidization, which is attributed to the nature of the equilibration of the PAA precursor with the respective anhydride- and amino-terminated species in the polycondensation. However, the anhydride ring would not be detected below 93 °C, suggesting that the anhydride ring is present either with very low concentration or in an open carboxylic acid form at temperatures less than 93 °C.

Fifth, structural evolution takes place as a three-step process: initiation, primary growth, and secondary growth. The initiation step begins at 132 °C, where the imidization reaction has only a 3.2% yield, and immediately the primary growth takes place up to 202 °C where the imidization reaction has a 91.0% yield. The secondary crystallization begins at 310 °C, the temperature at which imidization is complete, and continues with increasing temperature up to 380 °C. The secondary growth may take place favorably above $T_{g(onset)}$ (310 °C), even though the polymer chain mobility is limited because of its chain stiffness.

Sixth, the imidization-induced structural evolution may depend on the history of the molecular ordering in the preparation of the precursor film. Such domains of molecular order may act as nuclei in the imidization-induced structural evolution.

Seventh, for the crystalline structure formed by imidization, the thermal expansion coefficient along the lateral direction is estimated to be 61 ppm/°C over 25−200 °C and 158 ppm/°C over 310−380 °C.

Finally, the thermally imidized polymer film has a crystallinity of only 21.4%. This crystallinity level is accomplished by heating to 166 °C, where only 45.5% imidization has occurred. This temperature is still far below the final imidization temperature of 380 °C.

Acknowledgment. This study was supported by the Center for Integrated Molecular Systems (Korea Science & Engineering Foundation). The synchrotron X-ray diffraction measurement was supported by the Ministry of Science & Technology and POSCO.

LA0108656